Journal Name

RSCPublishing

ARTICLE

Synthesis of all-aliphatic polyamide dendrimers based on a 3,3´-diaminopivalic acid scaffold†

Cite this: DOI: 10.1039/x0xx00000x

Antonio Jesus Ruiz-Sanchez,[ab‡] Pablo Mesa-Antunez,[ab‡] Nekane Barbero,[ab] Daniel Collado,[ab] Yolanda Vida,[ab] Francisco Najera[ab] and Ezequiel Perez-Inestrosa*[ab]

Received ooth January 2012,
Accepted ooth January 2012

DOI: 10.1039/x0xx00000x

www.rsc.org/

Over recent years the importance of dendrimers has continued to increase in both life and material sciences. Multiple chemical strategies have been described toward the preparation of dendrimeric structures. Here, we present a new approach for the production of all-aliphatic polyamide dendrimers. In our approach, iterative 3,3'-diaminopivalic acid connections act as building blocks for dendrimer construction. 3,3'-Diazidopivalic acid units underpin a two-step pathway involving carboxylic acid-amine condensation, followed by azide reduction. The carboxylic acid-amine condensation step can be carried out by conventional methods, while the hydrogen-catalyzed azide-to-amine reduction is a clean process particularly appropriate for dendrimer preparation. Spectroscopic characterization of functionalized surface azides (Gn-N_3) and amines (Gn-NH_2) confirm the proposed structures. These dendrimers were studied in explicit solvent by atomistic forcefield-based molecular dynamics to characterize structural properties such as shape, radius and monomer distribution. Our results show that these compounds are similar in size and shape, with Gn-NH_2 having a slightly bigger size and exhibiting lower terminal unit backfolding.

Introduction

Increasing interest has focused on the use of polymer chemistry and nanotechnology for the development of new and improved materials. Extensive research into dendrimers and dendrons has resulted in a field that traverses chemistry, physics, biology and medicine. These branched molecules have found important applications in different fields ranging from material sciences to biomedicine. Moreover, as non-biological macromolecules, their primary structure has been developed to the same level of precision as biological molecules.

A key requirement for producing new dendrimeric materials with enhanced functions is the development of novel chemistries that can deliver the required degree of structural accuracy.[1–4]

Although some of the first wave of dendrimers developed have been successfully applied to different scientific areas (material, antennas, biomedical applications,[5–11] etc) and some recent dendrimeric structures have shown promise for specific applications,[12–15] full exploitation of their potential will require the development of more versatile molecules whose structure can be precisely tailored to suit their purpose.

Recently, we have demonstrated that a related family of dendrons has interesting properties for biomedical applications when supported over gold surfaces.[16] These promising results motivated us to design and synthesize a new family of alkyl-amide dendrimers i) formed from amide-linked subunits (polyamide dendrimers) ii) possessing surface azide groups that can be converted to readily functionalizable amines.

A number of aliphatic dendrimers combining a dendrimeric architecture with polyamide functions, such as polyamide amine (PAMAM) dendrimers, have been reported previously.[17–22] However, there have been relatively few reports using aliphatic polyamides in this context, lysine dendrimers being one example.[23] Although there are high expectations for the applications of dendrimers as new materials, many potential uses are limited because the commonly used synthesis approach requires a tedious procedure involving multistep protection and deprotection processes.

In general, dendrimers are synthesized from multifunctional monomers. In the case of a divergent dendrimer synthesis, each new dendrimer layer (i.e. generation) is added sequentially.[24] In this work, we present the development of a simple synthetic approach for a novel class of all aliphatic polyamide dendrimer consisting of the direct condensation of 3,3'-diazidopivalic acid (**1**) as an AB_2 building block. Carboxylic acid groups function to connect each monomeric subunit via amide linkages, while the presence of the azide groups in the form of "protected amines" (pro-amines) allows growth of the dendrimer to be controlled generation by generation.

Experimental Section

Materials

Chemicals and solvents were obtained from Sigma-Aldrich and Merck, and they were used as received without further purification unless stated (more detailed data are provided in the ESI†).

General Procedure for amide formation

A mixture of the corresponding amine, CH_2Cl_2 and 10% aqueous sodium hydroxide was cooled to 0 °C. 3,3'-Diazidopivalic acid chloride (**2**) was freshly prepared in CH_2Cl_2 and added dropwise while the temperature was kept to 0 ºC. After addition, the reaction was allowed to reach room temperature and stirred overnight. The organic layer was then separated, washed with 10% aqueous sodium hydroxide, 1 M aqueous HCl and water, dried over anhydrous $MgSO_4$ and the solvent removed. Purification by silica gel column chromatography gave the desired compound. For the preparation of **G3-N_3**, different conditions were used due to solubility problems. Compound **2** in dry DMF was slowly added over a mixture of **G2-NH_2** and DMAP in dry DMF under an argon atmosphere, and stirred at room temperature overnight. The solvent was removed and the residue dissolved in CH_2Cl_2. The organic layer was washed with 1 M aqueous HCl, 10% aqueous sodium hydroxide and water, dried over anhydrous $MgSO_4$ and the solvent removed. Purification by silica gel column chromatography gave the desired compound.

General Procedure for azide reduction

The corresponding azide derivative was dissolved in MeOH and the solution shaken under a hydrogen atmosphere (20 bar) in the presence of 10% Pd/C for 5 hours. The catalyst was filtered off through Celite® and washed with methanol. The filtrate was concentrated under vacuum to yield the desired compound as colorless oil in almost quantitative yield.

Molecular Dynamics Simulations

Simulations were performed using the AMBER12 MD software package.[25] Briefly, we utilized the AMBER force field parameters (parm99), for the azide group we used the parameter described before,[26] and those not included were transferred from the General Atom Force Field parameters (GAFF).[27] Initial dendrimer conformations were generated using the Dendrimer Building Tool (DBT).[28] The system was minimized and then heated to 300 K over 40 ps. Simulations were run at physiological pH (7.4) in NPT ensemble at 300 K and 1 atm for 20 ns. Non-bonded interactions were cutoff at 9 Å. Time steps of 2 fs were taken with implementation of the SHAKE routine.[29] Dendrimers were equilibrated for 2 ns and starting from these configurations, production runs of 20 ns trajectories were performed under an NPT ensemble. Trajectory analyses were performed using the Amber modules *ptraj* and *cpptraj*. Snapshots from the trajectories within this paper were created with VMD software.[30] Further details of the Molecular Dynamics Simulations are described in the ESI†.

Results and Discussion

Synthesis of AB_2 Building Block

We have designed a simple AB_2 monomer composed of a carboxylic acid and two amino groups that allows the preparation of dendrimers connected exclusively by amide bonds. As shown in Scheme 1, the dendrimers presented here are derived from the iterative binding of 3,3'-diaminopivalic acid monomers. The monomer's one acid and two azide groups allow us to grow dendrimer generations by amide bond formation.

This strategy requires preparing a derivative with conveniently protected amino functions and free carboxylic acid.[31] Several methods for protecting amines have been presented.[32] A convenient protecting group must be able to withstand acid group activation conditions while permitting amide bond formation, and further, its deprotection method should be compatible with amide functionalization.[33,34] The azide group presents all these desired features.[35,36] Addition of this functional group to a substrate can be easily achieved by a nucleophilic substitution reaction. Moreover, conversion to a primary amino group is feasible in very good yields by catalytic transformation and with little or no side products in organic solvent, thus making it easier to use in biological environments.[37] Furthermore, the possibility of using the Staudinger reduction reaction allows for its transformation into amines in the presence of other functional groups, such as alkenes and alkynes that are not compatible with catalytic hydrogenation.

Scheme 1 shows the synthesis of compound **1**, the monomeric unit which forms the basis for this dendrimer synthesis strategy. Starting from commercially available 3,3'-dichloropivalic acid, we obtained a 3,3'-diazidopivalic acid (**1**) derivative by reacting the former compound with sodium azide, in a dimethylformamide-water (10%) mixture to ensure sodium azide dissolution. This reaction proceeds with good, isolable yields of compound **1**, with multigram scale synthesis possible. Compound **1** is a 2,2-bis(aminomethyl)propanoic acid precursor since azide group reduction yields the corresponding amine function that is key for building the dendrimeric structure. Its carboxylic acid group allows the connection of monomeric subunits via amide linkages, while the presence of pro-amine azide groups allows dendrimer growth to be controlled from generation to generation.

Dendrimer Synthesis

Scheme 1 details the strategy proposed for dendrimer construction involving two iterative steps: i) condensation between **1** and either the dendrimer core, or surface amine groups of the corresponding dendrimer generation, obtaining amide-linked multi-azides, and ii) reduction of the multi-azide structure to its corresponding multi-amine form.

Journal Name

RSCPublishing

ARTICLE

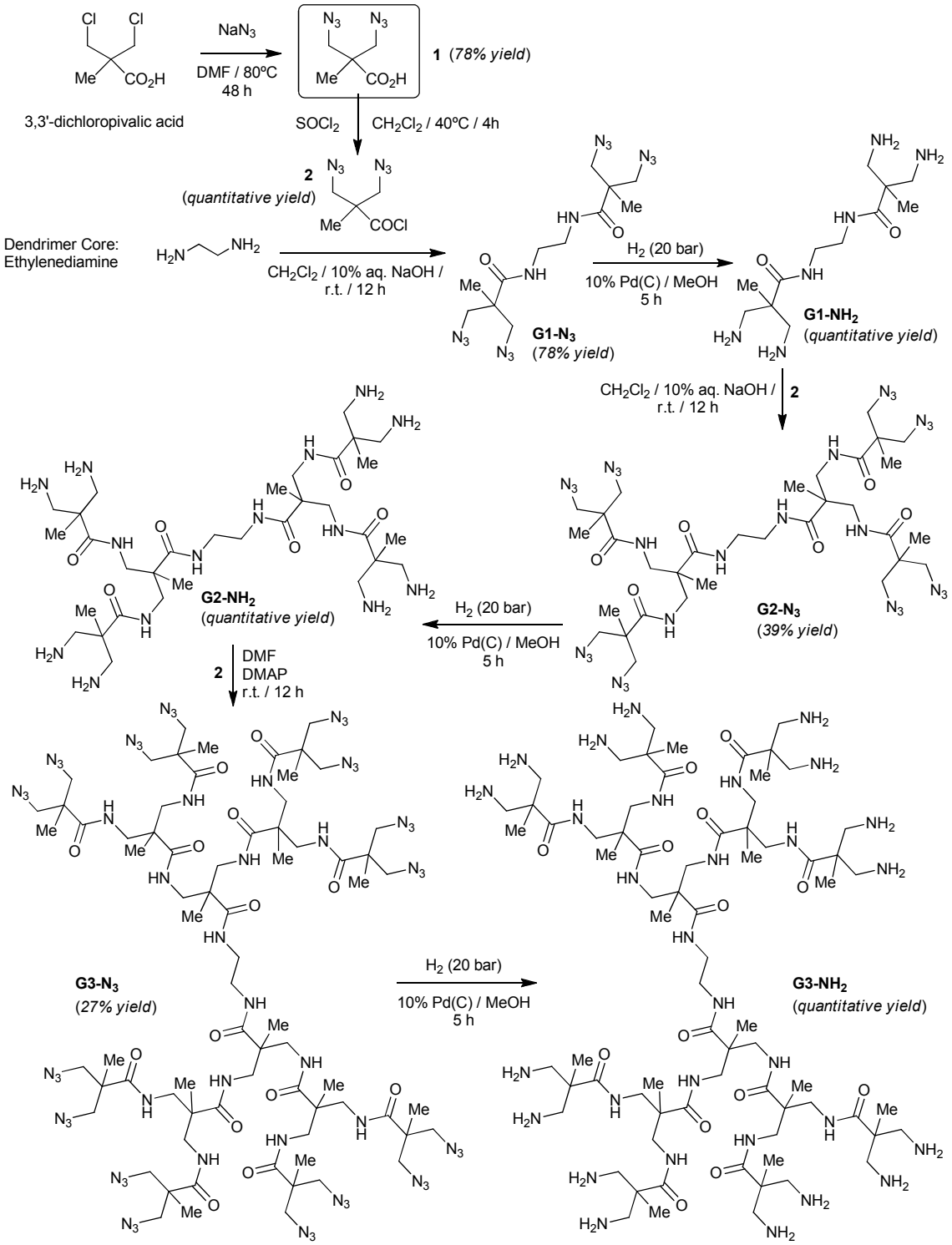

Scheme 1 Dendrimer Synthesis via Sequential Acylation-Hydrogenation Reactions

Journal Name

RSCPublishing

ARTICLE

Table 1 Molecular characteristics of the dendrimers

Dendrimer	Molecular Formula	Number of peripheral groups	Calculated exact mass	Experimental exact mass
G1-N_3	$C_{12}H_{20}N_{14}O_2$	4	393.19664	393.19645
G2-N_3	$C_{32}H_{52}N_{30}O_6$	8	953.47589	953.47893
G3-N_3	$C_{72}H_{116}N_{62}O_{14}$	16	1037.52082[a]	1037.51988
G1-NH_2	$C_{12}H_{28}N_6O_2$	4	289.23465	289.23527
G2-NH_2	$C_{32}H_{68}N_{14}O_6$	8	745.55190	745.55118
G3-NH_2	$C_{72}H_{148}N_{30}O_{14}$	16	1658.18600	1658.14900

[a] Calculated for $[M+2H]^{2+}$

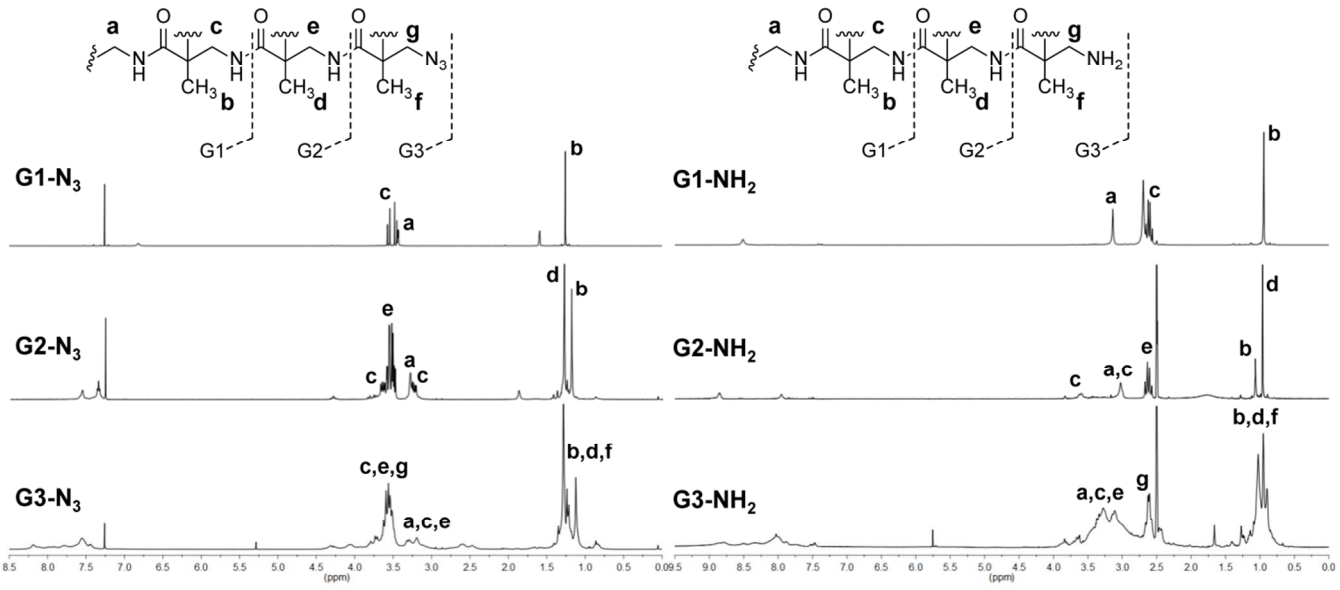

Fig. 1 ^{1}H-NMR spectra of the dendrimers Gn-N_3 ($CDCl_3$) (left), and Gn-NH_2 ($(CD_3)_2SO$) (right).

The condensation step can be performed by common methods used in the preparation of amides from carboxylic acids and amines. Here, we prepared the activated acid **1** derivative (compound **2**) and reacted it with ethylenediamine as the dendrimer-core, under Schotten–Baumann conditions to give the corresponding tetra-azide 1st generation dendrimer (**G1-N_3**).

For the reduction step, optimal results were obtained using catalytic hydrogenation conditions under H_2 atmosphere on Pd/C in MeOH.

This reduction reaction was carried out successfully with quantitative yields and without side product formation to produce **G1-NH_2**. Scheme 1 shows the iterative method use for dendrimer generation growth.

Gn-N_3 and Gn-NH_2 dendrimers were characterized by NMR, IR and Mass Spectrometry (MS). Their molecular characteristics are summarized in Table 1.

The ^{1}H NMR spectra of these dendrimers are shown in Fig. 1 (more detailed data are provided in the ESI†). As a general trend, the signals corresponding to azide-attached methylene protons, which appear as a group of signals centered at 3.60 ppm, are shifted to high field (around 2.50 ppm) when azide groups are reduced. Methylene protons in second and third generation dendrimers show a similar chemical shift with values in the 4.0 – 3.0 ppm region. Heteronuclear Multiple Quantum Coherence (HMQC) NMR was used to studied H,C correlation in **G2-N_3** and **G2-NH_2** dendrimers. These experiments enabled the correct assignment of methylene proton signals to their respective generations.

Changes in IR spectra can be used to monitor the azide-amine reduction reaction. Disappearance of the strong azide-associated signal at 2095 cm^{-1} confirms that each Gn-N_3 was efficiently transformed to the corresponding Gn-NH_2 dendrimer (Fig. 2). Finally, MS studies confirmed that the branching/functionalization steps of each dendrimer generation occurred quantitatively and selectively without side reactions, which is an important issue in the synthesis of dendrimers.

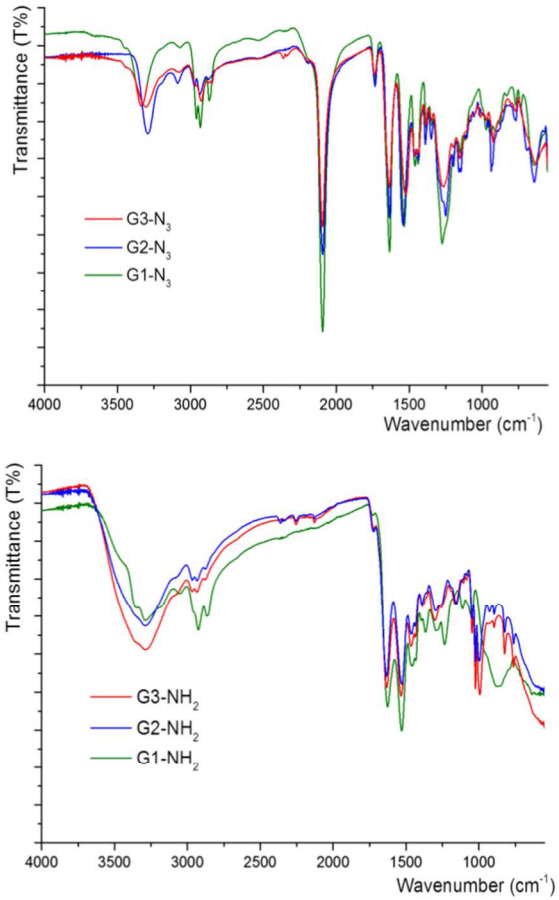

Fig. 2 Infrared spectra of Gn-N_3 (top spectra) and Gn-NH_2 (bottom spectra).

Fig. 1 shows the ^{1}H NMR spectra of **G1-N_3** and **G1-NH_2**, where all peaks could be unambiguously assigned. Methylene protons of these molecules are constitutionally non-equivalent and show different chemical shifts.

After **G1-N_3** azide function reduction, the methylene protons (3.47 and 3.44 ppm) and methyl group (1.26 ppm), all belonging to the branching agent, appear at 2.64, 2.58 and 0.95 ppm, respectively.

More relevant is the disappearance of the intense azide group-associated infrared band at 2095 cm^{-1}, indicating complete transformation to amine functionality (Fig. 2).

The ESI-TOF characterization of these samples fully corroborates the results of the ^{1}H NMR analysis. Our data clearly show that the proposed synthesis pathway can be used successfully for the iterative growth of dendrimer generations.

Next, starting with **G1-NH_2** we used our procedure to grow an additional dendrimer generation. **G1-NH_2** was treated with compound **2** under Schotten-Baumann conditions and the resulting **G2-N_3** product was easily purified by silica gel chromatography. The same conditions as those previously described were applied to obtain amine derivative of second generation dendrimer. Both compounds **G2-N_3** and **G2-NH_2** were unambiguously characterized, using HMQC-^{1}H-^{13}C NMR, mass spectrometry and infrared spectroscopy. The appearance of an infrared band at 2095 cm^{-1} confirmed the introduction of azide groups into the new dendrimer. Significantly, we obtained direct evidence of the formation of new amide bonds from peaks at 175.0 and 174.1 ppm of the ^{13}C NMR spectrum, corresponding to first and second generation amide bonds, respectively. Moreover, two singlet signals belonging to the branching monomer methyl groups of each generation (Fig. 1, peaks *b* and *d*), were clearly observed at 1.29 (G2) and 1.12 (G1) ppm in the ^{1}H NMR spectra and at 20.0 (G2) and 19.2 (G1) in the ^{13}C NMR spectra (Fig. S12 in ESI†). In the ^{1}H NMR of **G2-N_3**, four groups of signals overlap in the 3.0-4.0 ppm region. One corresponds to the ethylenediamine core molecule, (Fig. 1, peak *a* at 3.29 ppm). The signals showed two different types of protons that correlate with corresponding signals in the ^{13}C NMR spectrum, which were identified as the methylene protons of generation 1 (Fig. 1, peaks *c* at 3.65 and 3.25 ppm). The correlation between second generation methylene protons (Fig. 1, peaks *e*) with the corresponding ^{13}C NMR signal can be observed in the heteronuclear bidimensional NMR spectrum (Fig. S13 in ESI†). Finally, mass spectrometry ESI-TOF confirmed the molecular weight of the azido-derivative dendrimer. The terminal azide infrared band disappeared after catalytic hydrogenation of **G2-N_3**, indicating complete reduction of the azide groups to amines. The reaction yield was near quantitative and with adequate purity to be used without further purification. Characterization of **G2-NH_2** by HMQC NMR revealed two different signals, (Fig. S17 in ESI†, peaks *b* and *d*), assignable to the methyl protons of G1 and G2, at 1.06 and 0.92 ppm, respectively, high field shifted compared to corresponding azide-derivative dendrimer.

The sequence of reactions described above was repeated to generate a third generation dendrimer. The amine functions of **G2-NH_2** are available for branching reactions at the arm ends. However, the low solubility of this compound in dichloromethane reduces the formation of amide bonds and the efficiency of the Schotten-Baumann reaction. Therefore, the coupling reaction was optimized in monophasic conditions using DMAP in DMF and the resulting (**G3-N_3**) compound was characterized. The appearance of azide signals in the infrared spectrum at 2095 cm^{-1}, as well as ^{13}C NMR peaks at 176.0, 174.9 and 174.2 ppm attributable to the three different generations of amide groups, confirmed monomer incorporation. Dendrimer molecular weight was confirmed by MALDI-TOF mass spectrometry.

Journal Name

RSCPublishing

ARTICLE

Table 2 Aspect ratios, asphericities, Radius of gyration (R_g), Radius of the Solvent Accessible Surface Area (R_{SASA}) and Solvent Accessible Area of the dendrimers.[a]

Dendrimer	I_x/I_y	I_x/I_z	δ	R_g (Å)	R_{gNterm} (Å)[b]	R_{SASA} (Å)
G1-N_3	1.20 ± 0.08	2.52 ± 0.49	0.058 ± 0.019	3.96 ± 0.13	4.40 ± 0.39	5.53
G2-N_3	1.22 ± 0.09	1.79 ± 0.17	0.027 ± 0.008	5.70 ± 0.10	7.26 ± 0.22	8.16
G3-N_3	1.12 ± 0.05	1.65 ± 0.11	0.020 ± 0.005	7.63 ± 0.13	9.55 ± 0.31	11.27
G1-NH_2	1.04 ± 0.02	6.40 ± 1.80	0.146 ± 0.027	4.60 ± 0.32	5.44 ± 0.46	5.34
G2-NH_2	1.18 ± 0.08	4.10 ± 0.89	0.107 ± 0.021	7.03 ± 0.49	8.73 ± 0.54	8.14
G3-NH_2	1.11 ± 0.05	2.23 ± 0.28	0.047 ± 0.012	9.06 ± 0.17	11.05 ± 0.22	11.75

[a]Values averaged over the last 1 ns simulation run. Each snapshot was taken after 1 ps. [b]Respect to the azido group for the Gn-N_3 and to the amino group for Gn-NH_2 dendrimers.

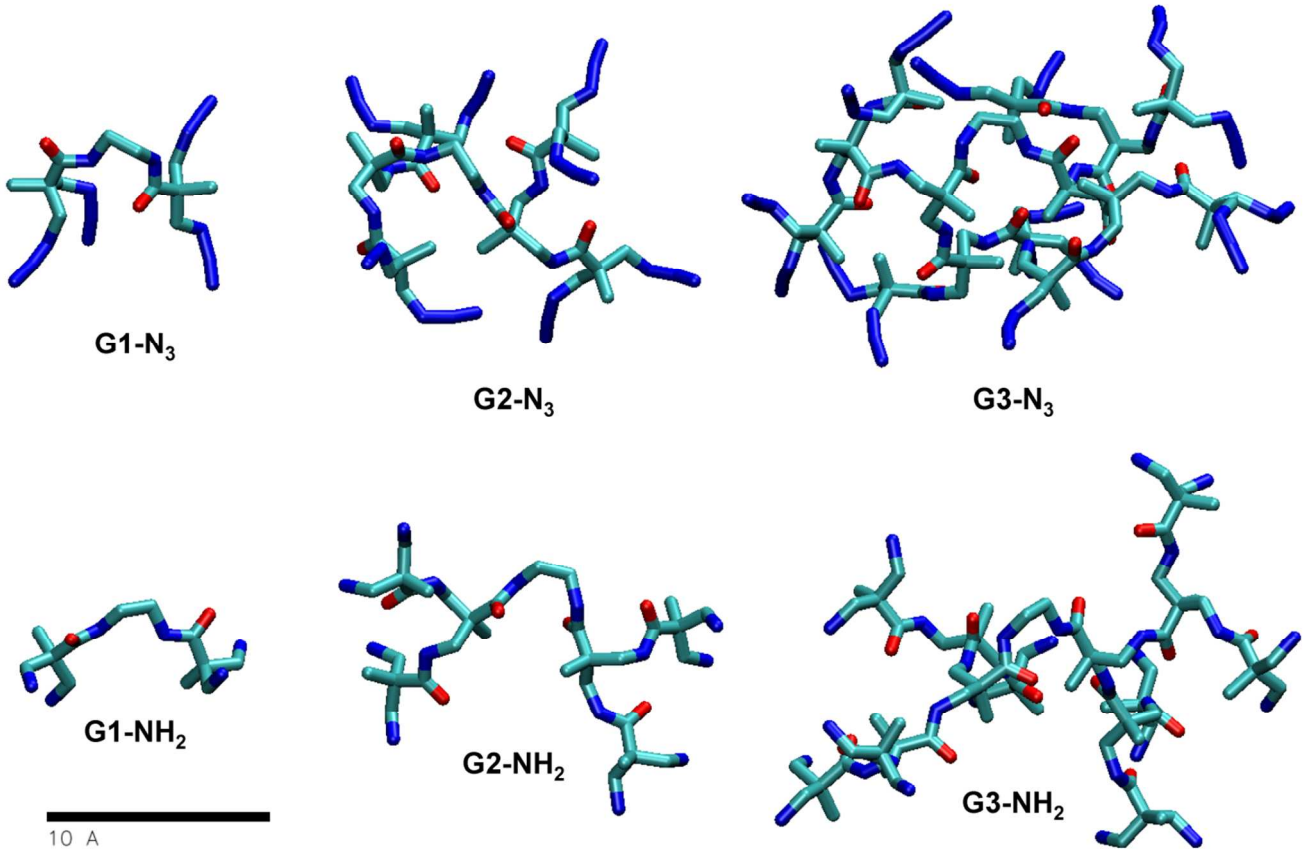

Fig. 3 Selected snapshots of Gn-N_3 and Gn-NH_2 dendrimers after MD simulations. To simplify the figure, hydrogen atoms have been omitted, carbon atoms shown in cyan, nitrogen atoms in blue and oxygen atoms in red.

Catalytic hydrogenation of this compound with palladium yielded **G3-NH_2** dendrimer with 16 amino groups in quantitative yields without side product formation. The azide band in the infrared spectrum (Fig. 2) was lost and the spectroscopic properties of **G3-NH_2** were consistent with those observed for lower dendrimer generations. Likewise, after azide group reduction, the peaks assigned to azide-linked methylene protons in ^{1}H NMR, became high field shifted ($\Delta\delta$= 0.3ppm) in the **G3-NH_2** dendrimer.

A thermal stability study was carried out and results demonstrated a sufficiently high thermal stability for storage and further processing up to 200 °C (Fig. S25 and S26 in ESI†).

Theoretical Calculations

In order to obtain information about the structure of these compounds, molecular models were created for generations 1 to 3 and simulated in explicit solvents (chloroform for Gn-N_3 and water for Gn-NH_2) using molecular dynamics.

Dendrimers were built with three different residues: the ethylenediamine core (COR), the branched repeating fragment (REP), and the terminal ends (TAZ) and (TAM) for Gn-N_3 and Gn-NH_2 dendrimers, respectively (Fig. S27 in ESI†).

The equilibrated structures of these molecules have also been analyzed and several properties calculated (Table 2): such as the Radius of gyration R_g, the solvent accessible surface area (SASA) and the radius obtained from its variations R_{SASA}, the aspect ratio, asphericities and finally their fractal dimensions.

We found that the size of these molecules increases with each generation, when measured in terms of R_g, (Fig. S29 in ESI†), with the Gn-NH_2 series being slightly bigger than the Gn-N_3 one. However, their R_{SASA} values, which can be considered to represent effective macromolecule size,[38] show that both series are similar in size and that even the larger number of terminal amine groups of higher generation **G3-NH_2** do not result in a significantly bigger molecule due to protonation of these terminal groups at physiological pH (Fig. S30 and S31 in ESI†). The back-folding of Gn-N_3 dendrimer terminal groups is indicated by R_{gNterm} values always consistently below 89% of R_{SASA}. In contrast, Gn-NH_2 molecules show a lower degree of back-folding of terminal amine groups toward the periphery of the molecules.

The relation between R_g and the number of dendrimer atoms, N, is an indication of a structure's space-filling (Fig. S32 in ESI†). The related fractal dimensionality value, d_f, takes account of the compactness of the dendrimer series, where a perfectly smooth spherical surface have a d_f = 3,[39] in our molecules this dimensionality values is 2.60 and 2.45 for Gn-N3 and Gn-NH_2 dendrimers respectively (Fig. S32 in ESI†). This indicates that these dendrimer generations do not form perfect spheres.

A structure-persistent characteristic of these dendrimers can be obtained from the average values of the three principal moments of inertia I_x, I_y, I_z (in descending order). I_x/I_y and I_x/I_z ratios (Table 2) are a measure of the dendrimer's ellipsoid shape eccentricity (Fig. S33 in ESI†). Gn-N_3 dendrimers showed I_x/I_y and I_x/I_z ratios of between 1.12-1.20 and 1.65-2.52, respectively. In contrast, Gn-NH_2 exhibited I_x/I_y ratios between 1.04-1.18 and I_x/I_z ratios in the range of 2.23-6.40. Thus, the aspect ratio I_x/I_y is very similar for both types of dendrimers, whereas I_x/I_z ratios decrease as a function of generation. This diminution is higher for Gn-NH_2 indicating that they have a more ellipsoidal shape than Gn-N_3 dendrimers. This is corroborated by their asphericity values (Fig. S33 in ESI†), which show that more globular structures only occur at higher generations. In all cases, the Gn-N_3 dendrimers are more spherical than the Gn-NH_2 due to the absence of charge on their surface.

Typical equilibrated conformations of the dendrimer generations are shown in Fig. 3. To simplify the figure, the hydrogen atoms have been omitted, the carbon atoms are depicted in cyan, nitrogen atoms in blue and oxygen atoms in red.

The distribution of atoms within the dendrimers can be described using radial density profiles. Curves corresponding to Gn-N_3 and Gn-NH_2 dendrimer generations are shown in Fig. S34 in ESI†. For all dendrimers, the maximum density is predicted to be close to the core of the molecules, decaying toward the edge. In the case of Gn-N_3, dendrimer atom density for generations 2 and 3 show minimums of around 3.1 Å, and then increase to maximums of 3.7 and 4.7 Å respectively. This indicates a region with high localization, low atom mobility and therefore with a dense dendrimer shell pattern.

In contrast, the radial distribution function for 2nd and 3rd generation Gn-NH_2 dendrimers is predicted to be higher in the inner core region, decaying slowly toward the molecule ends. This indicates a denser core region compared to the dendrimer mid-region. Finally, in the tail zone, the density decays monotonically toward the molecule ends.

The distribution of the different residues within dendrimer molecules is indicated by their radical distribution profiles (Fig. S34 in ESI†). In all dendrimers, COR monomers predicted to be close to the core. As the generation increases, the probability of finding a monomer, REP, TAZ or TAM, throughout the molecule also increases. The number of terminal monomers doubles with each generation, so the terminal azido or amine groups become spread over the molecule but always with increasing density toward the outer region of the dendrimer (Fig. 4).

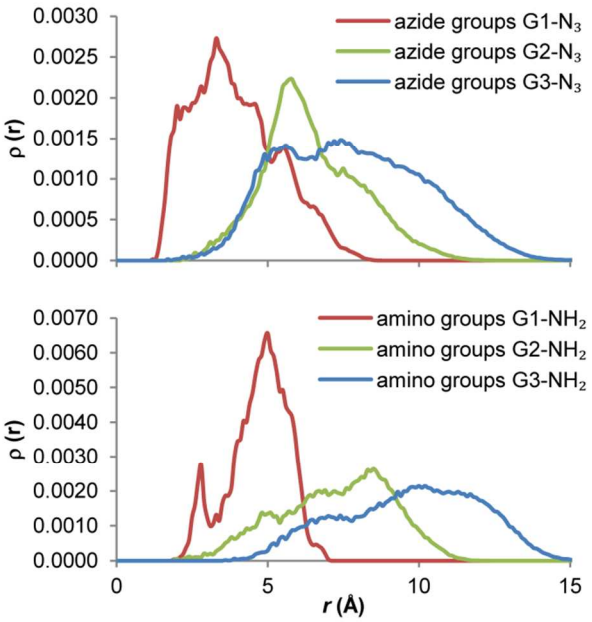

Fig. 4 Radial distribution function of terminal azido groups in Gn-N_3 (top) and terminal amino groups in Gn-NH_2 (bottom), using dendrimer center of mass as reference. The unit value for ρ(r) is expressed in atoms/Å^3.

These results indicate a higher degree of terminal monomer back-folding for Gn-N_3 with respect to the Gn-NH_2, where the

maximum density of protonated amine groups is consistent with the effective R_{SASA}, thus making these groups more exposed to the polar solvent.

Conclusions

In conclusion, 3,3'-diazidopivalic acid (**1**) can be efficiently employed as a building block to yield dendrimers with an all-aliphatic polyamide skeleton. Azido groups are effective as protected amines allowing the iterative growing of dendrimer generations. This strategy represents a facile synthetic method for aliphatic polyamide dendrimers based on a divergent approach. The spectroscopic characterization of the Gn-N_3 and Gn-NH_2 dendrimers confirms the structures obtained and the efficiency of the two-step condensation/reduction generation grow procedure. Gn-N_3 dendrimers are soluble in common organic solvents, whereas Gn-NH_2 dendrimers are soluble in aqueous media. While here we have shown that Gn-N_3 dendrimers are readily reduced to the corresponding Gn-NH_2, they can also be used as the basis of a series of new derivatives using copper(I)-catalyzed azide alkyne cycloaddition (CuAAC), the most common "click" reaction. Theoretical calculations of these dendrimers show that they are similar in size and shape, Gn-NH_2 having a slightly larger size and with very low back-folding of their terminal units.

Acknowledgements

This research was supported by different sources: Ministerio de Ciencia e Innovación-Spain (CTQ2010-20303 and CTQ2013-41339-P) and Junta de Andalucía-Spain (PI-0159/2013). RIRAAF (RD12/0013/0003). This research was co-financed by FEDER funds. We gratefully acknowledge the computer resources, technical expertise and assistance provided by the SCBI (Supercomputing and Bioinformatics) center of the University of Malaga.

Notes and references

[a] Universidad de Malaga, IBIMA, Department of Organic Chemistry, 29071-Malaga, Spain.
[b] Andalusian Centre for Nanomedicine and Biotechnology-BIONAND, Parque Tecnologico de Andalucia, 29590-Malaga, Spain.
‡ These authors contributed equally.
† Electronic Supplementary Information (ESI) available: Synthetic procedures, NMR spectroscopy, ESI-TOF MS, TGA analysis and extensive details about the simulation procedures used and its analysis. See DOI: 10.1039/b000000x/

1 M. V. Walter and M. Malkoch, *Chem. Soc. Rev.*, 2012, **41**, 4593–4609.
2 A. Carlmark, E. Malmström and M. Malkoch, *Chem. Soc. Rev.*, 2013, **42**, 5858–5879.
3 O. V. Borisov, A. A. Polotsky, O. V. Rud, E. B. Zhulina, F. a. M. Leermakers and T. M. Birshtein, *Soft Matter*, 2014, **10**, 2093–2101.
4 E. W. Meijer and M. H. P. van Genderen, *Nature*, 2003, **426**, 128–129.
5 V. Liljeström, J. Mikkilä and M. A. Kostiainen, *Nat. Commun.*, 2014, **5**.
6 S. Mignani, S. El Kazzouli, M. M. Bousmina and J.-P. Majoral, *Chem. Rev.*, 2014, **114**, 1327–1342.
7 J. Hu, T. Xu and Y. Cheng, *Chem. Rev.*, 2012, **112**, 3856–3891.
8 J. A. Hubbell, S. N. Thomas and M. A. Swartz, *Nature*, 2009, **462**, 449–460.
9 V. Percec, A. E. Dulcey, V. S. K. Balagurusamy, Y. Miura, J. Smidrkal, M. Peterca, S. Nummelin, U. Edlund, S. D. Hudson, P. A. Heiney, H. Duan, S. N. Magonov and S. A. Vinogradov, *Nature*, 2004, **430**, 764–768.
10 D. Astruc, *Nat. Chem.*, 2012, **4**, 255–267.
11 J. Lim, B. Turkbey, M. Bernardo, L. H. Bryant, M. Garzoni, G. M. Pavan, T. Nakajima, P. L. Choyke, E. E. Simanek and H. Kobayashi, *Bioconjug. Chem.*, 2012, **23**, 2291–2299.
12 S.-T. Lo, A. Kumar, J.-T. Hsieh and X. Sun, *Mol. Pharm.*, 2013, **10**, 793–812.
13 S. K. Yang, X. Shi, S. Park, T. Ha and S. C. Zimmerman, *Nat. Chem.*, 2013, **5**, 692–697.
14 G. Fuhrmann, A. Grotzky, R. Lukić, S. Matoori, P. Luciani, H. Yu, B. Zhang, P. Walde, A. D. Schlüter, M. A. Gauthier and J.-C. Leroux, *Nat. Chem.*, 2013, **5**, 582–589.
15 C. St-Pierre, M. Ouellet, D. Giguere, R. Ohtake, R. Roy, S. Sato and M. J. Tremblay, *Antimicrob. Agents Chemother.*, 2012, **56**, 154–162.
16 M. Soler, P. Mesa-Antunez, M.-C. Estevez, A. J. Ruiz-Sanchez, M. A. Otte, B. Sepulveda, D. Collado, C. Mayorga, M. J. Torres, E. Perez-Inestrosa and L. M. Lechuga, *Biosens. Bioelectron.*, 2015, **66**, 115–123.
17 D. A. Tomalia, H. Baker, J. Dewald, M. Hall, G. Kallos, S. Martin, J. Roeck, J. Ryder and P. Smith, *Polym. J.*, 1985, **17**, 117–132.
18 D. A. Tomalia, H. Baker, J. Dewald, M. Hall, G. Kallos, S. Martin, J. Roeck, J. Ryder and P. Smith, *Macromolecules*, 1986, **19**, 2466–2468.
19 D. A. Tomalia, A. M. Naylor and W. A. Goddard, *Angew. Chem. Int. Ed. Engl.*, 1990, **29**, 138–175.
20 D. A. Tomalia, H. D. Durst and Genealogically directed synthesis: Starburst/cascade dendrimers and hyperbranched structures, in *Supramolecular Chemistry I — Directed Synthesis and Molecular Recognition*, Springer Berlin Heidelberg, 1993, pp. 193–313.
21 J. M. J. Fréchet and D. A. Tomalia, *Dendrimers and other dendritic polymers*, Wiley, Chichester, 2001.
22 D. A. Tomalia, J. B. Christensen and U. Boas, *Dendrimers, Dendrons, and Dendritic Polymers: Discovery, Applications, and the Future*, Cambridge University Press, 2012.
23 U.S. Patent 4,289,872, 1981.
24 B. M. Rosen, C. J. Wilson, D. A. Wilson, M. Peterca, M. R. Imam and V. Percec, *Chem. Rev.*, 2009, **109**, 6275–6540.
25 D. A. Case, T. A. Darden, T. E. Cheatham, III, C. L. Simmerling, J. Wang, R. E. Duke, R. Luo, R. C. Walker, W. Zhang, K. M. Merz, B. P. Roberts, S. Hayik, A. E. Roitberg, G. Seabra, J. M. Swails, I. Kolossváry, K. F. Wong, F. Paesani, J. Vanicek, R. M. Wolf, J. Liu, X. Wu, S. R. Brozell, T. Steinbrecher, H. Gohlke, Q. Cai, X. Ye, J. Wang, M.-J. Hsieh, G. Cui, D. R. Roe, D. H. Mathews, M. G. Seetin, R. Salomon-Ferrer, C. Sagui, V. Babin, T. Luchko, S. Gusarov, A. Kovalenko and P. A. Kollman, *AMBER 12*, University of California, San Francisco, 2012.

26 A. T. P. Carvalho, P. A. Fernandes and M. J. Ramos, *Int. J. Quantum Chem.*, 2007, **107**, 292–298.
27 J. Wang, R. M. Wolf, J. W. Caldwell, P. A. Kollman and D. A. Case, *J. Comput. Chem.*, 2004, **25**, 1157–1174.
28 V. Maingi, V. Jain, P. V. Bharatam and P. K. Maiti, *J. Comput. Chem.*, 2012, **33**, 1997–2011.
29 J.-P. Ryckaert, G. Ciccotti and H. J. C. Berendsen, *J. Comput. Phys.*, 1977, **23**, 327–341.
30 W. Humphrey, A. Dalke and K. Schulten, *J. Mol. Graph.*, 1996, **14**, 33–38.
31 P. A. Wender, E. Kreider, E. T. Pelkey, J. Rothbard and C. L. VanDeusen, *Org. Lett.*, 2005, **7**, 4815–4818.
32 P. G. M. Wuts and T. W. Greene, *Greene's Protective Groups in Organic Synthesis*, Wiley-Interscience, Hoboken, N.J, 4 edition., 2006.
33 C. A. G. N. Montalbetti and V. Falque, *Tetrahedron*, 2005, **61**, 10827–10852.
34 E. Valeur and M. Bradley, *Chem. Soc. Rev.*, 2009, **38**, 606–631.
35 P. T. Nyffeler, C.-H. Liang, K. M. Koeller and C.-H. Wong, *J. Am. Chem. Soc.*, 2002, **124**, 10773–10778.
36 H. S. G. Beckmann and V. Wittmann, in *Organic Azides*, eds. S. Bräse and K. Banert, John Wiley & Sons, Ltd, 2009, pp. 469–490.
37 P. K. Sasmal, S. Carregal-Romero, A. A. Han, C. N. Streu, Z. Lin, K. Namikawa, S. L. Elliott, R. W. Köster, W. J. Parak and E. Meggers, *ChemBioChem*, 2012, **13**, 1116–1120.
38 Y. Liu, V. S. Bryantsev, M. S. Diallo and W. A. Goddard III, *J. Am. Chem. Soc.*, 2009, **131**, 2798–2799.
39 P. K. Maiti, T. Çağın, G. Wang and W. A. Goddard, *Macromolecules*, 2004, **37**, 6236–6254.

Iterative 3,3'-diaminopivalic acid connections act as building blocks in the production of new all-aliphatic polyamide dendrimers. 3,3’-Diazidopivalic acid units underpin a two-step pathway involving carboxylic acid-amine condensation, followed azide reduction.